Journal of Statistical Physics, Vol. 71, Nos. 3/4, 1993

Generalized Bethe Ansatz Solution of a One-Dimensional Asymmetric Exclusion Process on a Ring with Blockage

G. Schütz[1]

Received August 26, 1992; final October 28, 1992

We present a model for a one-dimensional anisotropic exclusion process describing particles moving deterministically on a ring of length L with a single defect, across which they move with probability $0 \leqslant p \leqslant 1$. This model is equivalent to a two-dimensional, six-vertex model in an extreme anisotropic limit with a defect line interpolating between open and periodic boundary conditions. We solve this model with a Bethe ansatz generalized to this kind of boundary condition. We discuss in detail the steady state and derive exact expressions for the current j, the density profile $n(x)$, and the two-point density correlation function. In the thermodynamic limit $L \to \infty$ the phase diagram shows three phases, a low-density phase, a coexistence phase, and a high-density phase related to the low-density phase by a particle–hole symmetry. In the low-density phase the density profile decays exponentially with the distance from the boundary to its bulk value on a length scale ξ. On the phase transition line ξ diverges and the current j approaches its critical value $j_c = p$ as a power law, $j_c - j \propto \xi^{-1/2}$. In the coexistence phase the width Δ of the interface between the high-density region and the low-density region is proportional to $L^{1/2}$ if the density $\rho \neq 1/2$ and $\Delta = 0$ independent of L if $\rho = 1/2$. The (connected) two-point correlation function turns out to be of a scaling form with a space-dependent amplitude $n(x_1, x_2) = A(x_2)\, r^{\kappa} e^{-r/\xi}$ with $r = x_2 - x_1$ and a critical exponent $\kappa = 0$.

KEY WORDS: Asymmetric exclusion process; Bethe ansatz; steady state; boundary-induced phase transitions; correlation functions.

1. INTRODUCTION

In statistical mechanics in two dimensions one model of particular interest has been the six-vertex model,[1,2] which was among the first to be solved exactly and which describes a wide variety of physical systems. Recently Kandel *et al.*[3] have shown that for a particular choice of vertex weights its

[1] Department of Nuclear Physics, Weizmann Institute, Rehovot, Israel.

822/71/3-4-8

diagonal-to-diagonal transfer matrix[2] describes a *one-dimensional* many-particle system with stochastic dynamics and hard-core repulsion such that each lattice site can be occupied by at most one particle. This is a class of models that has been studied in statistical mechanics for a long time,[4] but where only relatively few exactly soluble cases are known.[3,5] One of their interesting features is their close relationship to growth models[6] and (in the continuum) the KPZ equation[7] and the noisy Burgers equation.

The parameters in this class of diffusive systems can be chosen such that the model is symmetric, i.e., the probability of particles moving to the left is the same as that of moving to the right; or asymmetric, with different probabilities leading to a nonzero net current of particles in one direction. In the case of translational invariance, e.g., by imposing periodic boundary conditions, the system reaches a stationary state with constant density and the quantities of interest are density fluctuations and their correlations.[3,6,7] On the other hand, one can consider a system on a ring and break translational invariance by introducing a defect or inhomogeneity, a single pair of sites where the hopping probabilities of the particles are different from those on the other sites. In the language of growth models these are systems with a defect where the local growth rate differs from its bulk value (see refs. 8 and 9 and references therein). Considering an *asymmetric* model with a defect, one does not expect a uniform density any more, but a nontrivial density profile and, as numerical results show,[8–10] development of a shock front if parameters are chosen suitably. The interplay between the inhomogeneity and particle transport can lead to phase transitions even in these one-dimensional models with short-range interaction.

In this paper we present such a model defined on a ring with a defect and give an exact solution using Bethe ansatz methods, which have proven to be a powerful tool in the construction and investigation of exact solutions of two-dimensional integrable models such as the six-vertex model. We consider a fully asymmetric exclusion process with deterministic movement of particles in one direction everywhere except in one point, where the motion of the particles in this direction is probabilistic. The dynamics of the model is defined as follows: Each site x on the ring $(1 \leqslant x \leqslant L)$ is either occupied $[\tau_x(t) = 1]$ or empty $[\tau_x(t) = 0]$ at time t. The time evolution consists of two half time steps. In the first half step divide the ring with L sites (L even) into pairs of sites $(1, 2)$, $(3, 4)$,..., $(L-1, L)$. If both sites in a pair are occupied or empty or if site $2x-1$ is empty and site $2x$ occupied, they remain so at the intermediate time $t' = t + 1/2$. If site $2x-1$ is occupied and site $2x$ empty, then the particle moves with probability 1 to site $2x$, i.e.,

$$\begin{aligned} \tau_{2x-1}(t') &= \tau_{2x-1}(t)\, \tau_{2x}(t) \\ \tau_{2x}(t') &= \tau_{2x-1}(t) + \tau_{2x}(t) - \tau_{2x-1}(t)\, \tau_{2x}(t) \end{aligned} \tag{1.1}$$

These rules are applied in parallel to all pairs. In the second half step the pairing is shifted by one lattice unit such that the pairs are now $(L, 1)$, $(2, 3)$, etc. The same rules as before are applied in these pairs except in $(L, 1)$, where a particle on site L moves with probability $0 \leqslant p \leqslant 1$ to site 1 (if 1 was empty) and remains with probability $1-p$ on site L (again, if 1 was empty):

$$\begin{aligned}
\tau_L(t+1) &= 1 \quad \text{with probability} \\
&\quad p\tau_L(t')\,\tau_1(t') + (1-p)\,\tau_L(t') \\
\tau_L(t+1) &= 0 \quad \text{with probability} \\
&\quad p[1-\tau_L(t')\,\tau_1(t')] + (1-p)[1-\tau_L(t')] \\
\tau_1(t+1) &= 1 \quad \text{with probability} \\
&\quad \tau_1(t') + p\tau_L(t')[1-\tau_1(t')] \\
\tau_1(t+1) &= 0 \quad \text{with probability} \\
&\quad 1-\tau_1(t') - p\tau_L(t')[1-\tau_1(t')]
\end{aligned} \tag{1.2}$$

In the mapping of ref. 3 this is equivalent to a two-dimensional, four-vertex model in thermal equilibrium with a defect line where a fifth vertex has nonvanishing Boltzmann weights. The two steps describing the motion of particles define the diagonal-to-diagonal transfer matrix in the vertex model (see Section 2). The pairing is chosen as in ref. 3, but the hopping probabilities are different.

This limiting case of the anisotropic six-vertex model might appear not very interesting due the deterministic movement of the particles in the bulk. But it turns out that the defect causes particles to pile up (because of the hard-core repulsion) and, depending on the total density, to cause phase transitions between a low-density phase to a coexistence phase with a low- and a high-density region and finally to a high-density phase as in fully probabilistic models. The phase transitions from the coexistence phase to the low- and high-density phases are related by a particle–hole symmetry (see Section 2).

Another surprise is its solvability, which cannot be expected from this defect-type boundary condition. So far, Bethe ansatz solutions for vertex models are known only for free boundary conditions with surface fields and for certain twisted toroidal boundary conditions depending on the global symmetry of the system.[2,11] In particular, Gwa and Spohn discussed a Bethe ansatz solution of a probabilistic fully asymmetric exclusion process with periodic boundary conditions and derived the large-L behavior of some of the energy gaps which are relevant for the dynamical scaling exponent for the stationary correlations of the noisy Burgers equation.[12] In our case a Bethe ansatz calculation as in these known cases of boundary conditions is not possible. However, we will show that judiciously chosen new basis vectors allow for a Bethe ansatz solution with a new kind of boundary condition on the Bethe wave function. The ansatz in this basis gives rise to Bethe ansatz equations different from those obtained in the case of the usual integrable twisted or free boundary conditions.

The paper is organized as follows. In Section 2 we discuss some of the symmetries of the model which help in finding this basis. Then, in Section 3 we proceed to compute the eigenvectors to nonzero eigenvalues of the transfer matrix. Some of the calculations and proofs for this section are given in the Appendix. In Section 4 we study in detail the steady state and give an exact expression for the average occupation as a function of the site x on the ring of the blockage strength p. We establish the presence of a phase transition as announced above and compute the critical density as a function of p. In particular, we discuss the current, the density profile of the system, and the steady-state correlation functions in the various phases. In Section 5 we compare the phase diagram and density profile obtained in Section 4 with other asymmetric exclusion models with blockage and draw some conclusions.

2. SYMMETRIES OF THE FINITE SYSTEM

In this section we translate the model described above into the language of the six-vertex model following ref. 3, and discuss some of its symmetries. The transfer matrix derived below is used in the Bethe ansatz diagonalization in Section 3.

Consider the six-vertex model on a diagonal square lattice defined as follows: Place an up- or down-pointing arrow on each link of the lattice and assign a nonzero Boltzmann weight to each of the vertices shown in Fig. 1. (All other configurations of arrows around an intersection of two lines, i.e., all other vertices, are forbidden.) The partition function is the sum of the products of Boltzmann weights of a lattice configuration taken over all allowed configurations.

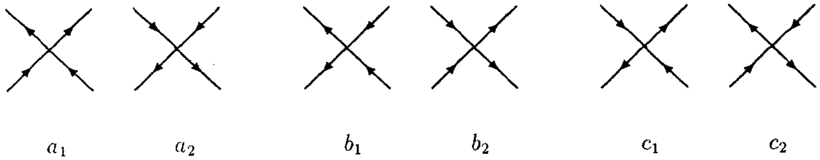

Fig. 1. Allowed vertex configurations in the six-vertex model and their Boltzmann weights as given in (2.1). Up-pointing arrows correspond to particles, down-pointing arrows represent vacant sites. In the dynamical interpretation of the model the Boltzmann weights give the transition probability of the state represented by the pair of arrows below the vertex to that above the vertex.

In the transfer matrix formalism up- and down-pointing arrows as shown in Fig. 1 in each row of a diagonal square lattice built by M of these vertices represent the state of the system at some given time t. Corresponding to the M vertices there are $L = 2M$ sites in each row. The configuration of arrows in the next row above (represented by the upper arrows of the same vertices) then corresponds to the state of the system at an intermediate time $t' = t + 1/2$, and the configuration after a full time step $t'' = t + 1$ corresponds to the arrangement of arrows two rows above. Therefore each vertex represents a local transition from the state given by the lower two arrows of a vertex representing the configuration on sites j and $j + 1$ at time t to the state defined by the upper two arrows representing the configuration at sites j and $j + 1$ at time $t + 1/2$. The correspondence of the vertex language to the particle picture used in the introduction can be understood by considering up-pointing arrows as particles occupying the respective sites of the chain while down-pointing arrows represent vacant sites, i.e., holes.

The diagonal-to-diagonal transfer matrix T acting on a chain of L sites (L even) of the general asymmetric six-vertex model with vertex weights $a_1, \ldots, c_1$ as shown in Fig. 1 is then defined by[2]

$$T = \prod_{j=1}^{L/2} T_{2j} \cdot \prod_{j=1}^{L/2} T_{2j-1} = T^{\text{even}} T^{\text{odd}} \tag{2.1}$$

The matrices T_j act nontrivially on sites j and $j + 1$ in the chain; on all other sites they act as the unit operator. All matrices T_j and $T_{j'}$ with $|j - j'| \neq 1$ commute. For an explicit representation of the transfer matrix we choose a spin-1/2 tensor basis where the Pauli matrix σ_j^z acting on site j of the chain is diagonal and spin down at site j represents a particle (up-pointing arrow) and spin up a hole (down-pointing arrow). In this basis $\tau_j = \frac{1}{2}(1 - \sigma_j^z)$ is the projection operator on particles on site j and $s_j^{\pm} = \frac{1}{2}(\sigma_j^x \pm i\sigma_j^y)$($\sigma^{x,y,z}$ are the Pauli matrices) create (s_j^-) and annihilate (s_j^+) particles, respectively. The matrices T_j in this basis are defined by

$$T_j = \begin{pmatrix} a_2 & 0 & 0 & 0 \\ 0 & c_1 & b_2 & 0 \\ 0 & b_1 & c_2 & 0 \\ 0 & 0 & 0 & a_1 \end{pmatrix}_{j,j+1} \tag{2.2}$$

The dynamics of our model is encoded in the transfer matrix by choosing the vertex weights as follows:

$$\begin{aligned} &\text{bulk:} && a_1 = a_2 = 1 \quad b_1 = 0,\ b_2 = 1 \quad c_1 = 1,\ c_2 = 0 \\ &\text{defect line:} && a_1' = a_2' = 1 \quad b_1' = 0,\ b_2' = p \quad c_1' = 1,\ c_2' = 1 - p \end{aligned} \tag{2.3}$$

In the bulk this leads to

$$T_j = 1 + s_j^+ s_{j+1}^- - \tau_j(1-\tau_{j+1}) = \begin{pmatrix} 1 & 0 & 0 & 0 \\ 0 & 1 & 1 & 0 \\ 0 & 0 & 0 & 0 \\ 0 & 0 & 0 & 1 \end{pmatrix}_{j,j+1} \tag{2.4}$$

In the particle language the matrices T_j describe the local transition probabilities of particles moving from site j to site $j+1$ represented by the corresponding vertices. If sites j and $j+1$ are both empty or occupied, they remain as they are under the action of T_j. The same holds for a hole on site j and a particle on site $j+1$, corresponding to the diagonal elements of T_j, representing vertices a_1, a_2, and c_1. If there is a particle on site j and a hole on site $j+1$, the particle will move with probability one to site $j+1$. This accounts for vertex b_2.

As discussed in the introduction, we assume periodic boundary conditions, i.e., we identify site $L+1$ with site 1, but we consider a defect on the boundary allowing for vertex c_2. In terms of local transition probabilities this means that we allow for a movement of particles with probability $p \neq 1$ from site L to site 1. Therefore T_L is given by

$$T_L(p) = 1 + p[s_L^+ s_1^- - \tau_L(1-\tau_1)] = \begin{pmatrix} 1 & 0 & 0 & 0 \\ 0 & 1 & p & 0 \\ 0 & 0 & 1-p & 0 \\ 0 & 0 & 0 & 1 \end{pmatrix}_{L,1} \tag{2.5}$$

The transfer matrix $T = T(p)$ acts parallel first on all odd–even pairs of sites $(2j-1, 2j)$, then on all even–odd pairs. Thus, in the first half time step T^{odd} shifts particles from the odd sublattice to the even sublattice (so far not occupied) and then, in the second half step, T^{even} moves particles from the even sublattice to the odd sublattice again. As a result, we expect an asymmetry in the average occupation of the even and odd sublattices which is related to the particle current. In a model with transfer matrix $\tilde{T} = T^{\text{odd}} T^{\text{even}}$ the asymmetry will be reversed, but there will be no essential difference in the physical properties of these two systems.

The limiting cases $p=0$ and $p=1$ play a special role. If $p=1$ (no blockage), one has periodic boundary conditions and translational invariance, and we will denote the transfer matrix $T(p=1)$ by T^P, while $p=0$ (total blockage) corresponds to free boundary conditions with no interaction between sites L and 1. For later convenience we denote $T(p=0)$ by T^F. The matrix $T(p)$ interpolates continuously between free and periodic boundary conditions; one has $T(p) = pT^P + (1-p)\, T^F$.

Having defined the transfer matrix, we discuss some of its symmetries. We will denote by

$$|x_1, x_2,..., x_N\rangle = s^-_{x_1} s^-_{x_2} \cdots s^-_{x_N} |\cdot\rangle$$

the N-particle state with particles on sites $x_1,..., x_N$ ($|\cdot\rangle$ is the state with all spins up corresponding to no particle). The number operator

$$N = \sum_{j=1}^{L} \tau_j, \qquad [T, N] = 0 \tag{2.6}$$

commutes with T, splitting the transfer matrix into sectors of fixed numbers of particles.

The parity operator P reflects particles with respect to the center of the chain located between sites $x = L/2$ and $x = L/2 + 1$ and is defined by

$$P\,|x_1, x_2,..., x_N\rangle = |L+1-x_N,..., L+1-x_2, L+1-x_1\rangle \tag{2.7}$$

The charge conjugation operator

$$C = \prod_{j=1}^{L} \sigma_j^x \tag{2.8}$$

interchanges particles and holes and therefore turns an N-particle state into a state with $L - N$ particles. One finds

$$[T, CP] = 0 \tag{2.9}$$

N and CP generate an $O(2)$ symmetry of the transfer matrix that allows us to restrict our discussion to $0 \leqslant N \leqslant L/2$.

The conserved current associated to the conservation law (2.6) is obtained from the commutators of τ_{2x} and τ_{2x-1} with T, which turn out to play a crucial role in the construction of the eigenstates of the transfer matrix in the next section. Defining the projector on holes at site x as

$$\sigma_x = 1 - \tau_x \tag{2.10}$$

and the current operators j^{even}_{2x}, j^{even}_{L}, and j^{odd}_{2x-1} by

$$\begin{aligned} &j^{\text{odd}}_{2x-1} = \tau_{2x-1}\sigma_{2x} \qquad (\text{all } x) \\ &j^{\text{even}}_{2x} = (1-\sigma_{2x-1}\sigma_{2x})(1-\tau_{2x+1}\tau_{2x+2}) \qquad (x \neq L/2) \\ &j^{\text{even}}_{L} = p(1-\sigma_{L-1}\sigma_L)(1-\tau_1\tau_2) \end{aligned} \tag{2.11}$$

a straightforward calculation yields ($x \neq L/2$)

$$\begin{aligned}
[T, \tau_{2x}] &= T[\tau_{2x} - (1 - \sigma_{2x-1}\sigma_{2x})\,\tau_{2x+1}\tau_{2x+2}] \\
&= j_{2x}^{\text{even}} - j_{2x-1}^{\text{odd}} \\
[T, \tau_{2x+1}] &= T[\tau_{2x+1}\sigma_{2x+2} - \tau_{2x-1}\sigma_{2x} - \tau_{2x} \\
&\quad + (1 - \sigma_{2x-1}\sigma_{2x})\,\tau_{2x+1}\tau_{2x+2}] \\
&= j_{2x+1}^{\text{odd}} - j_{2x}^{\text{even}}
\end{aligned} \tag{2.12}$$

and at the boundary

$$\begin{aligned}
[T, \tau_L] &= T[\tau_L - (1 - \sigma_{L-1}\sigma_L)\,\tau_1\tau_2] \\
&\quad - (1-p)\,T^F(1 - \sigma_{L-1}\sigma_L)(1 - \tau_1\tau_2) \\
[T, \tau_1] &= T[\tau_1\sigma_2 - \tau_{L-1}\sigma_L - \tau_L + (1 - \sigma_{L-1}\sigma_L)\,\tau_1\tau_2] \\
&\quad + (1-p)\,T^F(1 - \sigma_{L-1}\sigma_L)(1 - \tau_1\tau_2)
\end{aligned} \tag{2.13}$$

From these commutation relations we obtain

$$\begin{aligned}
[T, \tau_{2x} + \tau_{2x+1}] &= T(j_{2x+1}^{\text{odd}} - j_{2x-1}^{\text{odd}}) \qquad (\text{all } x) \\
[T, \tau_{2x-1} + \tau_{2x}] &= T(j_{2x}^{\text{even}} - j_{2x-2}^{\text{even}}) \qquad (x \neq 1, L/2) \\
[T, \tau_{L-1} + \tau_L] &= T^P \cdot j_L^{\text{even}} - T \cdot j_{L-2}^{\text{even}} \\
[T, \tau_1 + \tau_2] &= T \cdot j_2^{\text{even}} - T^P \cdot j_L^{\text{even}}
\end{aligned} \tag{2.14}$$

Current conservation implies that the expectation values of the current operators j_{2x}^{even} and j_{2x-1}^{odd} do not depend on x, $\langle j_{2x}^{\text{even}} \rangle = \langle j_{2x-1}^{\text{odd}} \rangle = \text{const} = j$, and denoting the density of particles N/L by ρ, CP invariance gives $j(\rho) = j(1-\rho)$. From the definition of the current operator j_L in (2.11) we see that in the steady state j is bounded from above by p, but on the other hand, we expect it to increase with the number of particles in the chain. This already indicates the possibility of a phase transition for $p < 1$ as the density increases. That a phase transition does indeed occur will be shown in Section 4.

3. GENERALIZED BETHE ANSATZ SOLUTION

We now turn to the task of finding the eigenvectors and eigenvalues of $T(p)$. A few general remarks are in place. First it should be noted that T is not a symmetric matrix; therefore, one has to compute left and right eigenvectors separately. Left and right eigenvectors with eigenvalue Λ will be denoted $\langle\Lambda|$ and $|\Lambda\rangle$, respectively, with the corresponding "wave functions" $\Phi_\Lambda(x_1,..., x_N)$ and $\Psi_\Lambda(x_1,..., x_N)$. They are defined by

$$\begin{aligned} |\Lambda\rangle &= \sum_{x_1,...,x_N} \Psi_\Lambda(x_1,..., x_N)\,|x_1, x_2,..., x_N\rangle \\ \langle\Lambda| &= \sum_{x_1,...,x_N} \Phi_\Lambda(x_1,..., x_N)\langle x_1, x_2,..., x_N| \end{aligned} \tag{3.1}$$

where $\langle x_1, x_2,..., x_N|$ is the transpose of the column vector $|x_1, x_2,..., x_N\rangle$ in the sector of N particles. The sum runs over all different sets of coordinates $\{x_1,..., x_N\}$, $1 \leqslant x_i \leqslant L$, in a chain of L sites. The wave function does not depend on the order of its arguments.

Second, since T is a matrix of transition probabilities where the sum of all entries in each column is 1 for any value of p, $\sum_m (T(p))_{m,n} = 1$, its largest eigenvalue is 1 with an (unnormalized) *left* eigenvector $\langle 1|$. The corresponding unnormalized wave function is constant, $\Phi_1(x_1,..., x_N) = 1$ for all configurations $(x_1,..., x_N)$, $1 \leqslant x_i \leqslant L$:

$$\langle 1| = \sum_{x_1,...,x_N} \langle x_1, x_2,..., x_N| \tag{3.2}$$

This particular eigenvector does not depend on p. In what follows we will compute only *right* eigenvectors; the computation of the corresponding left eigenvectors proceeds along similar lines.

Third, it should be mentioned that T is not fully diagonalizable, i.e., the number of linearly independent eigenvectors is smaller than the dimension of T. However, the subspace with nonzero eigenvalues is diagonalizable. That is, to each root $\Lambda \neq 0$ of the characteristic polynomial of $T(p)$ there exists an eigenvector. It is easy to construct some eigenvectors to eigenvalue 0, but there is no *complete* set of eigenstates. We restrict our calculations to the set of eigenvectors with nonzero eigenvalue, since, from the physical point of view, these are the relevant ones.

T^P is a special limiting case of the general six-vertex model in the diagonal-to-diagonal transfer matrix approach, which can be solved exactly using the Bethe ansatz with a wave function

$$\begin{aligned} B(x_1,..., x_N) &= \sum_{\mathscr{P}} (-1)^P\, b_{p_1,...,p_N} \prod_{m=1}^{N} B_{p_m}(x_m) \\ b_{1,...,N} &= \prod_{1 \leqslant m < n \leqslant N} b_{mn} \end{aligned} \tag{3.3}$$

This is a sum of products of N single-particle wave functions

$$B_j(x_m) = \begin{cases} F_1(k_j) \exp ik_j x_m & x_m \text{ odd} \\ F_2(k_j) \exp ik_j x_m & x_m \text{ even} \end{cases} \tag{3.4}$$

The two-body phase shift functions $b_{mn} = b(k_m, k_n)$ and the ratio F_1/F_2 are determined by the interaction between the particles.[13] The sum runs over all permutations $\mathscr{P} = (p_1,..., p_N)$ of the numbers $(1,..., N)$ and $(-1)^P$ denotes the sign of the permutation. The N quantum numbers k_m characterizing different wave functions with eigenvalues $\Lambda = \Lambda(k_1,..., k_N) = \Lambda(k_1) \cdots \Lambda(k_N)$ are determined from the boundary conditions imposed on the system. The existence of such a solution is due to the integrability of this system, leading to an infinite set of conserved charges in the infinite system. The transfer matrix of the generic (periodic) six-vertex model is soluble with this Bethe ansatz for a class of twisted boundary conditions and, with some modification, for free boundary conditions with certain surface fields,[2,11] but no solution in the case of the defect-type periodic boundary conditions considered here is known. We will show that in the fully asymmetric limit defined by the Boltzmann weights (2.3) the model even with this defect is soluble with a Bethe ansatz.

In order to solve this problem, we will further study the implications of the symmetries discussed in the preceding section. This will allow us to identify an invariant right subspace of $T(p)$ and to restrict the Bethe ansatz to this subspace. Properly chosen boundary conditions on the wave function yield a solution to the problem and it turns out that the eigenvectors are still given by a set of quantum numbers $k_1,..., k_N$. As discussed in the preceding section, CP invariance allows us to restrict ourselves to $0 \leqslant N \leqslant L/2$.

3.1. Periodic Boundary Conditions (No Blockage)

The translationally invariant case $p = 1$ is most easily solved by noting the following:

1. T^P has an invariant (right) subspace with particles placed only on odd lattice sites.

This can be proven as follows: Consider a state with only odd sites occupied. First, T^{odd} [See (2.1)] will move *all* particles to their neighboring even sites since they were all vacant; then T^{even} shifts this configuration again one site further,

$$T^P \, |2x_1 - 1,..., 2x_N - 1\rangle = |2x_1 + 1,..., 2x_N + 1\rangle \tag{3.5}$$

so that the resulting state still has particles only on the odd sublattice.

On this subspace of dimension

$$d_N(L) = \binom{L/2}{N}, \qquad (0 \leqslant N \leqslant L/2) \tag{3.6}$$

T^P acts as translation operator, causing all particles to move with the same velocity around the ring, and the eigenvalues are

$$\Lambda_n = \exp(4\pi i n/L), \qquad 0 \leqslant n \leqslant L/2 - 1 \tag{3.7}$$

All eigenvalues are degenerate in each sector with fixed N (but $N \neq 0, 1, L/2 - 1, L/2$) since any vector of the form

$$|\Lambda_n\rangle = \sum_{j=0}^{L/2-1} \Lambda_n^{-j} \,|2x_1 - 1 + 2j, 2x_2 - 1 + 2j, ..., 2x_N - 1 + 2j\rangle \tag{3.8}$$

has eigenvalue Λ_n. [There is no degeneracy in the special cases $N = 0$ (no particle) and $N = L/2$ (all odd sites occupied), since the dimensions of these subspaces are $d_0(L) = d_{L/2}(L) = 1$, and in the cases $N = 1$ or $N = L/2 - 1$ where the dimensions are $d_1(L) = d_{L/2-1}(L) = L/2$. In the latter case each of the eigenvalues (3.7) occurs once.]

Furthermore, we find:

2. The eigenvectors obtained in this way are the only eigenvectors with $\Lambda \neq 0$.

In the Appendix we prove that if $p = 1$,

$$\tau_{2x}\sigma_{2y-1}\,|\Lambda\rangle = 0 \qquad \text{if} \quad \Lambda \neq 0 \tag{3.9}$$

This proves that any eigenfunction $\Psi(x_1, ..., x_N)$ not vanishing for all even x_i must have eigenvalue $\Lambda = 0$: Suppose $\Psi(x_1, ..., 2x, ..., x_N) \neq 0$, i.e., there is a particle on an even site $2x$ in some state contributing to $|\Lambda\rangle$. Then (3.9) can be satisfied only if *all* $L/2$ odd sites in this state are occupied as well. This means that $N > L/2$, in contradiction to the assumption $N \leqslant L/2$.

A Bethe ansatz calculation would give the same result, of course, with $F_2(k_m) = 0$ [see (3.4)] and the constants b_{mn} defined in (3.3) arising from the interaction left undetermined. The eigenstates can be considered as sets of noninteracting particles with fixed relative distances all moving around the ring with constant velocity 1. All these "frozen" states have one internal degree of freedom, leading to the excitations (3.8) with momentum $4\pi n/L$. The interaction between particles on the odd and even sublattices accounting for a nontrivial behavior of the system is, so to speak, hidden, because it is such that all particles are forced onto the odd sublattice. States with particles on the even sublattice have eigenvalue 0 and therefore decouple.

Expectation values $\langle O\rangle$ of operators O in the steady state are defined by $\langle 1|\, O\, |1\rangle / \langle 1 | 1\rangle$, where $\langle 1|$ and $|1\rangle$ are the linear combinations of all eigenvectors with eigenvalue 1 with equal weight.[2] $\langle 1|$ is given by (3.2) and

$$|1\rangle = \sum_{x_1,\dots,x_N} |2x_1 - 1, 2x_2 - 1,\dots, 2x_N - 1\rangle \tag{3.10}$$

In particular, for the current (2.11) one obtains

$$j = \langle j^{\text{odd}}_{2x-1}\rangle = \langle \tau_{2x-1}\rangle = 2N/L = 2\rho \qquad (\rho \leqslant \tfrac{1}{2}) \tag{3.11}$$

3.2. Free Boundary Conditions (Full Blockage)

If $p = 0$, the system is even more trivial than in the translationally invariant case. All particles are moved to the boundary, where they get stuck and pile up. There is only a single eigenvector with $\Lambda \neq 0$, the steady state

$$|1\rangle = |L - N, L - N + 1,\dots, L\rangle \tag{3.12}$$

with eigenvalue $\Lambda = 1$. No current is flowing, $j = 0$, independent of ρ.

3.3. Partial Blockage ($0 < p < 1$)

Here the system shows nontrivial behavior. However, it turns out that the commutation relations (2.12) and (2.13) generate a large number of relations between the amplitudes $\Psi(x_1,\dots, x_N)$ for different arguments $(x_1,\dots, x_N)$. In the Appendix we prove that the wave function with k of its N arguments even (here labeled by $2x_i$) is given by the wave function of N odd sites (labeled by $2y_i + 1$):

$$\begin{aligned}\Psi_\Lambda(&2x_1,\dots, 2x_k, 2y_1 + 1,\dots, 2y_{N-k} + 1)\\ &= \left(\frac{1-p}{p}\right)^k \cdot \chi(2x_1,\dots, 2x_k, 2y_1 + 1,\dots, 2y_{N-k} + 1)\\ &\quad \times \Psi_\Lambda(2\tilde{y}_1 + 1,\dots, 2\tilde{y}_k + 1, 2y_1 + 1,\dots, 2y_{N-k} + 1)\end{aligned} \tag{3.13}$$

where $\Lambda \neq 0$ is assumed and

$$\tilde{y}_i = L/2 - x_i \tag{3.14}$$

[2] This definition is arbitrary and corresponds to a special choice of initial condition in the averaging. We select this particular state since it is the one obtained from the nondegenerate perturbed steady state ($p \neq 1$) by adiabatically switching off the perturbation ($p \to 1$, see below).

$\chi(x_1,..., x_N)$ is a step function taking the values 0 or 1 and is defined by the rules **3A–3D** below. In formulating these rules we adopt the following language. If *any* of the arguments x_i of χ takes a specific (even or odd) value x, $1 \leqslant x \leqslant L$, we say there is a particle at site x (because in this case χ is part of the amplitude of a state with site x occupied). On the other hand, if none of the arguments takes this specific value, we speak of the presence of a hole at site x. In this terminology $\chi(x_1,..., x_N)$ is defined as follows:

3. $\chi = 0$ if and only if there is a particle on an even site $2x$ and one of the following conditions holds:

A. There is a hole on site $2y+1$, with $2 \leqslant 2x < 2y+1 \leqslant L-1$.

B. There is a particle on site $L+1-2x$, with $2 \leqslant 2x \leqslant L$.

C. There are holes on site $2y+1$ and site $L-2y$ with $2 \leqslant 2x \leqslant L-2$, $2x < 2y+1 \leqslant L-1$.

D. $2 \leqslant 2x \leqslant L-N$.

These rules together with (3.13) define a new invariant subspace of dimension $d_N(L)$ as given in (3.6).

Straightforward calculation shows that the wave function with all its arguments x_i odd, but

$$(x_1,..., x_N) \neq (1, 3,..., 2j-1, x_{j+1},..., x_{N-2j}, L-2j+1,..., L-3, L-1)$$
$$\text{for some} \quad j, \qquad 1 \leqslant 2j-1 \leqslant N-1$$

can be found from an ansatz

$$\Psi_\Lambda(x_1,..., x_N) = B_\Lambda(x_1,..., x_N) \tag{3.15}$$

where B_Λ is a Bethe wave function (3.3) of an eigenvector with eigenvalue

$$\Lambda = \prod_{m=1}^{N} \Lambda_m, \qquad \Lambda_m = \exp - 2ik_m \tag{3.16}$$

and with boundary conditions

$$\begin{aligned} &B_\Lambda(1, 3,..., 2j-1, x_{j+1},..., x_{N-2j}, L-2j+1,..., L-3, L-1) \\ &\quad = p^{-j}\Lambda^j B_\Lambda(1, 3, 5,..., 4j-1, x_{j+1}+2j,..., x_{N-2j}+2j) \end{aligned} \tag{3.17}$$

In Eqs. (3.15) and (3.17) we assume the arguments of B to be ordered, $1 \leqslant x_1 < x_2 < \cdots < x_N \leqslant L-1$.

The phase shift functions b_{mn} defined in (3.3) are given by

$$b_{mn} = 1 - \Lambda_m^{-1} \tag{3.18}$$

and $F_1(k_m)=1$, $F_2(k_m)=0$ for all m. As in the usual Bethe ansatz, the boundary conditions give rise to a set of equations determining A_m, $m=1,..., N$:

$$pA_m^{-L/2}=[1-(1-p)\,A_m^{-1}](-1)^{N-1}\prod_{m=1}^{N}\frac{b_{mn}}{b_{nm}} \tag{3.19}$$

We see that changing the interaction in a single lattice site is sufficient to "revive" the interaction between nearest neighbors on the even and odd sublattices which is hidden in the translationally invariant case. As a consequence, the phase-shift functions (3.18) arising from this interaction are no longer undetermined and the system shows nontrivial behavior.

Equation (3.19) represents a set of N equations for N unknown quantities $A_m=\exp -ik_m$ involving powers of $L/2$ of A_m. One solution is easy to find; it is the steady state with

$$\begin{aligned} A(k_1,..., k_N)&=A_1=\cdots=A_N=1\\ B(x_1,..., x_N)&=1 \end{aligned} \tag{3.20}$$

for

$$(x_1,..., x_N)\neq(1, 3,..., 2j-1, x_{j+1},..., x_{N-2j}, L-2j+1,..., L-3, L-1)$$

and (3.21)

$$B_A(1, 3,..., 2j-1, x_{j+1},..., x_{N-2j}, L-2j+1,..., L-3, L-1)=p^{-j}$$

Other solutions have $A_m\neq 1$, $A_m\neq A_n$ for all m, n. For $p\neq 1$ the state with eigenvalue 1 is nondegenerate.

4. DISCUSSION OF THE STEADY STATE

4.1. Computation of the Average Occupation Number

Rule **3D** states that $\tau_{2x}\,|A\rangle=0$ for $2\leqslant 2x\leqslant L-N$. Therefore the steady-state current $j=\langle\tau_{2x-1}-\tau_{2x-1}\tau_{2x}\rangle$ [see (2.11)] is equal to the average occupation number $\langle\tau_{2x-1}\rangle$ on the odd sublattice in the range $1\leqslant 2x-1\leqslant L-N$. In this area particles move with velocity 1. Current conservation and the upper bound on the current discussed in Section 2 imply that also the density in this region is constant and bounded from above by p. On the other hand, in the region $L-N<2x-1\leqslant L-1$ one has $\langle\tau_{2x-1}\tau_{2x}\rangle\geqslant 0$ and consequently $\langle\tau_{2x-1}\rangle\geqslant j$. Here the defect causes the particles to move with average velocity less than 1 and one observes a nontrivial density profile. In order to study these two areas, we compute the average occupation number $n(x) = \langle 1 | \tau_x | 1 \rangle / \langle 1 | 1 \rangle$.

First we have to compute $\mathscr{F}_{L,N}(p) = \langle 1 | 1 \rangle$, which because of the form of the left eigenvector $\langle 1|$ of (3.2) is just the steady-state wave function summed over all its arguments,

$$\mathscr{F}_{L,N}(p) = \langle 1 | 1 \rangle = \sum_{x_1,\dots,x_N} \Psi_1(x_1,\dots,x_N) \tag{4.1}$$

It is convenient to normalize the right eigenfunction by taking $B(2x_1 - 1,\dots, 2x_N - 1) = p^N$ [with $(2x_1 - 1, 2x_N - 1) \neq (1, L-1)$] instead of $B(2x_1 - 1,\dots, 2x_N - 1) = 1$ as in (3.20). As a result of this normalization, the steady-state wave function contains only positive powers of p. Evaluating (4.1) then amounts to counting the multiplicity of all powers of p up to p^N in this sum, which is a combinatorial problem.

One way of solving this problem is to group the amplitudes $\Psi_1(x_1,\dots, x_N)$ into sets distinguished by their number $j = k/2$ of pairs of particles, which are defined as follows $(0 \leqslant k \leqslant N)$: We consider as a 0-pair any ordered, purely odd configuration $(x_1 < x_2 \cdots < x_N)$ with $x_1 \neq 1$:

$$k=0: \qquad (x_1,\dots, x_N), \qquad x_1 \neq 1 \tag{4.2}$$

while 1/2-pairs are the ordered configurations (x_i odd)

$$k=1: \qquad \left.\begin{matrix} (1, x_1,\dots, x_{N-1}) \\ (x_1,\dots, x_{N-1}, L) \end{matrix}\right\} \quad x_1 \neq 1 \quad \text{and} \quad x_{N-1} \neq L-1 \tag{4.3}$$

The 1-pairs are all ordered configurations (x_i odd)

$$k=2. \qquad \left.\begin{matrix} (1, x_1,\dots, x_{N-2}, L-1) \\ (x_1,\dots, x_{N-2}, L-1, L) \end{matrix}\right\} \quad x_1 \neq 1, 3 \tag{4.4}$$

while 3/2-pairs are the ordered configurations (x_i odd)

$$k=3: \qquad \left.\begin{matrix} (1, 3, x_1,\dots, x_{N-3}, L-1) \\ (3, x_1,\dots, x_{N-3}, L-1, L) \\ (1, x_1,\dots, x_{N-3}, L-2, L-1) \\ (x_1,\dots, x_{N-3}, L-2, L-1, L) \end{matrix}\right\} \quad \begin{matrix} x_1 \neq 1, 3 \\ \text{and } x_{N-3} \neq L-3 \end{matrix} \tag{4.5}$$

The 2-pairs are the ordered configurations (again, x_i odd)

$$k=4: \qquad \left.\begin{matrix} (1, 3, x_1,\dots, x_{N-4}, L-3, L-1) \\ (3, x_1,\dots, x_{N-4}, L-3, L-1, L) \\ (1, x_1,\dots, x_{N-4}, L-3, L-2, L-1) \\ (x_1,\dots, x_{N-4}, L-3, L-2, L-1, L) \end{matrix}\right\} \quad x_1 \neq 1, 3, 5 \tag{4.6}$$

Higher $k/2$-pairs are constructed analogously. We see that there are 2^m different kinds of k-pairs with $k = m - l/2$, $l = 0, 1$. They are distinguished by the arrangement of particles on even lattice sites. The number s_k of each kind of $k/2$-pair given by all possible arrangements of particles $(x_1,..., x_{N-k})$ on the unspecified odd sites is

$$s_k = \binom{L/2 - 1 - k}{N - k} \tag{4.7}$$

According to (3.13), which expresses the amplitudes with some arguments even in terms of amplitudes with purely odd arguments, the total contribution of all such 2^m kinds of pairs of type k to $\mathscr{F}_{L,N}(p)$ is p^{N-k}. Adding over all pairs of type k, one finds

$$\mathscr{F}_{L,N}(p) = \sum_{k=0}^{N} \binom{L/2 - N - 1 + k}{k} p^k \tag{4.8}$$

It is convenient to define the quantity $\gamma_k = s_{N-k} p^k$ and to introduce the incomplete β-function

$$\begin{aligned} I_{1-p}(L/2 - N, R + 1) &= (1-p)^{L/2-N} \sum_{k=0}^{R} \gamma_k \\ &= (1-p)^{L/2-N} \sum_{k=0}^{R} \binom{L/2 - N + R}{k} p^k (1-p)^{R-k} \\ &= (1-p)^{L/2-N} f_{L,N}(R; p) \end{aligned} \tag{4.9}$$

In terms of this function one has $\mathscr{F}_{L,N}(p) = f_{L,N}(N; p)$.

In the same way one can obtain an expression for

$$\mathscr{G}_{L,N}(x; p) = \langle 1 | \tau_x | 1 \rangle = \sum_{y_1,..., y_{N-1}} \Psi_1(y_1,..., y_{N-1}, x) \tag{4.10}$$

(Remember that the value of the wave function Ψ does not depend on the order of its arguments.) In order to compute $\mathscr{G}_{L,N}(x; p)$, one considers the same groups of amplitudes and counts powers of p with the additional restriction that one particle occupies site x. Taking $x = L - 2m$, the result is

$$\mathscr{G}_{L,N}(L - 2m; p) = (1-p) \sum_{k=0}^{N-2m-1} \gamma_k \tag{4.11}$$

while for x odd, $x = L - 2m - 1$, one obtains

$$\mathscr{G}_{L,N}(L - 2m - 1; p) = \sum_{k=0}^{N-2m-2} \gamma_k + p \sum_{k=\max(0, N-2m-1)}^{N-1} \gamma_k \tag{4.12}$$

Equations (4.11) and (4.12) can be written in closed form,

$$\mathscr{G}_{L,N}(x;\,p)=p\left|\sin\frac{\pi}{2}x\right|f_{L,N}(N-1;\,p)$$
$$+(1-p)\,f_{L,N}(N-L-1+x;\,p) \qquad (4.13)$$

So with $n(x)=\mathscr{G}_{L,N}(x;\,p)/\mathscr{F}_{L,N}(p)$ and $f^{(0)}=f_{L,N}(N-1;\,p)/f_{L,N}(N;\,p)$ we obtain an exact expression for the occupation number $n(x)$, which is the main result of this subsection:

$$n(x)=p\left|\sin\left(\frac{\pi}{2}x\right)\right|f^{(0)}+(1-p)\frac{f_{L,N}(N-L-1+x;\,p)}{f_{L,N}(N;\,p)} \qquad \left(\rho\leqslant\frac{1}{2}\right) \qquad (4.14)$$

The first quantity in this expression vanishes on the even sublattice and is constant on the odd sublattice. It reflects the anisotropy between the even and odd sublattices in this model. The second part describes the density profile; it is 0 for $x\leqslant L-N$. Since for $1\leqslant 2x-1\leqslant L-N$ one has $j=n(2x-1)$, we find the current

$$j=pf^{(0)}=p\frac{f_{L,N}(N-1;\,p)}{f_{L,N}(N;\,p)} \qquad (4.15)$$

Due to CP invariance (2.9), the average occupation number at density $\rho=N/L$ satisfies $n_{1-\rho}(x)=1-n_\rho(L+1-x)$.

4.2. The Phase Diagram

Having found the density distribution along the chain, we are in a position to determine the various phases of the system. We start by discussing some special cases which are easy to derive from (4.9). If $p=1$ (no blockage), one has

$$j=f^{(0)}=\frac{f_{L,N}(N-1;\,1)}{f_{L,N}(N;\,1)}=\binom{L/2-1}{N-1}\bigg/\binom{L/2}{N}=2\rho \qquad (4.16)$$

and the density $n(x)=|\sin(\tfrac{1}{2}\pi x)|\,f^{(0)}$ is uniform, but different on the even and odd sublattices,

$$n(x)=\begin{cases}2\rho & x\text{ odd}\\ 0 & x\text{ even}\end{cases} \qquad (4.17)$$

On the other hand, if $p=0$ (full blockage), then $j=0$ and the average occupation number is a step function,

$$n(x)=\begin{cases}1 & x>L-N\\ 0 & x\leqslant L-N\end{cases} \tag{4.18}$$

These two results were already obtained in Section 3.

Three more special cases are the two trivial limiting cases $\rho=0$ and $\rho=1$ and the half-filled system $\rho=1/2$. For $\rho=0$ we have $n(x)=0$ and for $\rho=1$ we have $n(x)=1$. In both cases the current is zero. For the half-filled system, Eq. (4.9) gives $f_{L,L/2}(R;p)=1$ if $R\geqslant 0$ and $f_{L,L/2}(R;p)=0$ if $R<0$. The resulting current is $j=p$ and one obtains the density profile

$$n(x)=\begin{cases}0 & x \text{ even}, \quad 2\leqslant x\leqslant L/2\\ p & x \text{ odd}, \quad 1\leqslant x\leqslant L/2-1\\ 1-p & x \text{ even}, \quad L/2+2\leqslant x\leqslant L\\ 1 & x \text{ odd}, \quad L/2+1\leqslant x\leqslant L-1\end{cases} \tag{4.19}$$

Here for any value of p the system is in a coexistence phase with a low-density region, $x\leqslant L/2$, and a high-density region, $x>L/2$.

From these examples we can already recognize the three different phases of the system and qualitatively draw the phase diagram. There is a low-density phase (I), a coexistence phase (II), and, through the particle–hole symmetry (2.9), a high-density phase (III) (see Fig. 2). Restricting ourselves to $\rho\leqslant 1/2$, we find that at $p=0$ the system is in the coexistence phase, while at $p=1$ it is in the low-density phase, independent of ρ. Note that in all these special cases the shape of the density profile does not depend on the size of the system.

In order to determine the phase transition line separating phases I and II, we consider the continuum limit $L\to\infty$, ρ and p fixed. We denote $s=k/N$ and $\gamma_k=\gamma(s)$. First we notice that

$$\begin{aligned}\frac{\gamma_k}{\gamma_{k-1}}&=\frac{p}{s}\left(\frac{2\rho-1}{2\rho}+s-\frac{1}{N}\right)\\ &=p\left(1+\frac{1-2\rho}{2\rho s}\right)+O\left(\frac{1}{L}\right)\end{aligned} \tag{4.20}$$

and therefore $\gamma(s)$ has a maximum at

$$s_0=\frac{p}{2\rho}\frac{1-2\rho}{1-p} \tag{4.21}$$

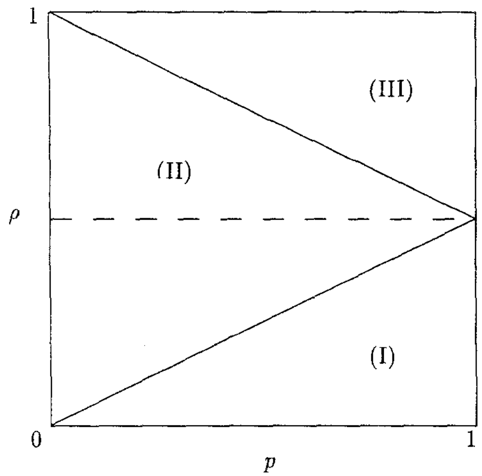

Fig. 2. Phase diagram of the model in the ρ–p plane. Region I is the low-density phase, region II the coexistence phase, and region III the high-density phase. The phases are separated by the curves $\rho = p/2$ and $\rho = 1 - p/2$, respectively. The dashed line $\rho = 1/2$ marks the half-filled system, which is in the coexistence phase for all $p < 1$. The lower and upper half-planes in this diagram are related by the particle–hole symmetry (2.8).

To the normalization $\mathscr{F}_{L,N}(p)$ of (4.8) only those $\gamma(s)$ with $0 \leqslant s \leqslant 1$ contribute, so the largest γ contributing to $\mathscr{F}_{L,N}(p)$ is $\gamma(1) = \gamma_N$ if $p \geqslant 2\rho$ (in this case the maximum $s_0 \geqslant 1$ is outside the range $0 \leqslant s \leqslant 1$) and $\gamma(s_0)$ if $p < 2\rho$. If L becomes very large and $1 \ll N$, $1 \ll L/2 - N$, one obtains from Stirling's formula

$$\gamma(s) = \frac{(1-2\rho)^{1/2}}{(\pi L)^{1/2}\,[1-(1-s)\,2\rho]^{1/2}\,(2\rho s)^{1/2}} \times \left[\left(\frac{p}{2\rho s}\right)^{2\rho s} \frac{[1-(1-s)\,2\rho]^{1-(1-s)2\rho}}{(1-2\rho)^{1-2\rho}}\right]^{L/2} \tag{4.22}$$

$$\gamma(1) = \frac{(1-2\rho)^{1/2}}{(\pi L)^{1/2}\,(2\rho)^{1/2}} \left[\left(\frac{p}{2\rho}\right)^{2\rho} (1-2\rho)^{2\rho-1}\right]^{L/2} \tag{4.23}$$

and

$$\gamma(s_0) = \frac{1-p}{(\pi L)^{1/2}\,[p(1-2\rho)]^{1/2}}\,[(1-p)^{2\rho-1}]^{L/2} \tag{4.24}$$

We first discuss the case $p > 2\rho$. In the continuum limit $L \to \infty$ the quantities $\gamma(s)/\gamma(1)$ vanish for $s < 1$ if the difference $1 - s$ is larger than of order $1/L$. Therefore, only the quantities $\gamma(s)$ with s infinitesimally close to 1 give a contribution to the sum $f_{L,N}(N-L-1+x; p)$ appearing in the expression for the density profile (4.14). After rescaling the length of the chain to 1 and defining the scaled distance r from the boundary as $r=(L-x)/L$ we arrive at the conclusion that the rescaled average occupation number $\tilde{n}(r)=\lim_{L\to\infty} n(L-Lr)$ vanishes for all finite (i.e., noninfinitesimal) distances r on the even sublattice and becomes a constant $\tilde{n}=2\rho$ on the odd sublattice (we keep $\rho=N/L$ fixed). This is the low-density phase (I) with

$$j=pf^{(0)}=2\rho \tag{4.25}$$

The total density on the even sublattice vanishes,

$$\rho^{\text{even}}=\lim_{L\to\infty} 2/L \sum_{x=1}^{L/2} n(2x)=0 \tag{4.26}$$

while

$$\rho^{\text{odd}}=\lim_{L\to\infty} 2/L \sum_{x=1}^{L/2} n(2x-1)=2\rho \tag{4.27}$$

However, if p is smaller than 2ρ (phase II), then the $\gamma(s)$ with s infinitesimally close to s_0 give nonvanishing contributions to $f_{L,N}(N-L-1+x; p)$ in (4.14) and consequently $\tilde{n}(r)$ will jump at $r_0=\rho(1-s_0)$ from p to 1 on the odd sublattice and from 0 to $1-p$ on the even sublattice. In this phase one finds

$$j=p \tag{4.28}$$

and

$$\begin{aligned} \rho^{\text{even}} &= (1-p)\, r_0=\tfrac{1}{2}(2\rho-p) \\ \rho^{\text{odd}} &= p(1-r_0)+r_0=\tfrac{1}{2}(2\rho+p) \end{aligned} \tag{4.29}$$

The curve $p=2\rho$ marks the phase transition between phases I and II and we denote the critical density $\rho=p/2$ by ρ_{crit}.

The phase diagram in the j–p plane is given in Fig. 3. Note that a similar phase diagram was obtained numerically in ref. 8 for a fully probabilistic asymmetric exclusion process. At fixed blockage strength p the current j increases in phase I with the density, $j=2\rho$, until the critical density is reached with $j=p$. Further increasing the density does not change the current until the density approaches its upper critical value $\tilde{\rho}_{\text{crit}}=$

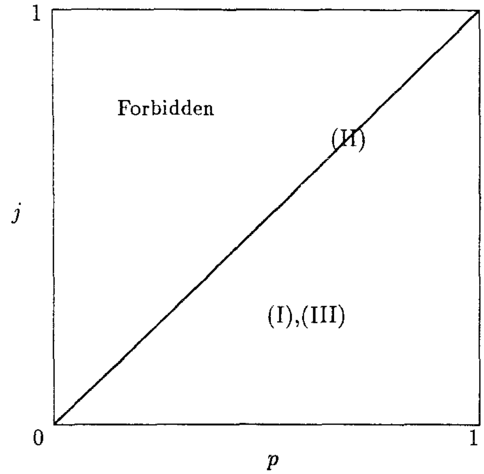

Fig. 3. Phase diagram of the model in the j–p plane. The curve $j=p$ represents the coexistence phase II, where $\rho_{\rm left}=1-\rho_{\rm right}$. In the area below one has $\rho_{\rm left}=\rho_{\rm right}$ corresponding to the asymptotically uniform phases I and III [see (4.31)]. The system cannot be stationary in the region above $j=p$ since the blockage imposes an upper bound p on the current the system can support.

$1-\rho_{\rm crit}$ and the system enters the uniform high-density phase, where $j=2(1-\rho)$. Taking the average occupation number between neighboring sites $\bar{n}(2x)=[n(2x-1)+n(2x)]/2$, we define in the continuum limit $\rho_{\rm left}=\bar{n}(r)$, $0<r<r_0$, and $\rho_{\rm right}=\bar{n}(r)$, $r_0<r<1$. In the three phases one has

$$\begin{aligned} &\rho_{\rm left}=\rho_{\rm right}<\rho_{\rm crit} && \text{phase I}\\ &\rho_{\rm left}=1-\rho_{\rm right}=1-\rho_{\rm crit} && \text{phase II}\\ &\rho_{\rm left}=\rho_{\rm right}>1-\rho_{\rm crit} && \text{phase III}\end{aligned} \tag{4.30}$$

4.3. Density Profile in Finite Systems

Now we turn to a discussion of the density profiles in phases I and II in large but finite systems. Throughout this subsection we assume that $0<\rho<1/2$ and $0<p<1$.

4.3.1. Low-Density Phase $p>2\rho$. We assume that the system is not close to the phase transition line $p=2\rho$ and therefore quantities of order $(2\rho/p)^N$ are exponentially small in N and are neglected in all calculations below. We first compute the current $j=\langle\tau_{2x-1}\rangle-\langle\tau_{2x-1}\tau_{2x}\rangle$. This quantity is independent of x and by choosing $x=1$ turns out to be the anisotropy $pf^{(0)}$ between the two sublattices,

$$j=p\frac{f_{L,N}(N-1;p)}{f_{L,N}(N;p)}=p\left(1-\frac{\gamma_N}{f_{L,N}(N;p)}\right) \tag{4.31}$$

Up to order $1/L$ one obtains

$$\begin{aligned}\frac{f_{L,N}(N;p)}{\gamma_N}&=\sum_{k=0}^{N}\frac{\gamma_k}{\gamma_N}\\ &=\sum_{k=0}^{N}\left\{\left(\frac{2\rho}{p}\right)^k-\frac{2}{L}\left[\frac{1-2\rho}{p}\frac{k(k-1)}{2}\left(\frac{2\rho}{p}\right)^{k-1}-k\left(\frac{2\rho}{p}\right)^k\right]\right\}\\ &=\frac{p}{p-2\rho}\left(1-\frac{2}{L}\frac{2\rho(1-p)}{(p-2\rho)^2}\right)\end{aligned} \tag{4.32}$$

Together with (4.31), this gives

$$j=2\rho\left(1-\frac{2}{L}\frac{1-p}{p-2\rho}\right) \tag{4.33}$$

In order to compute the density profile near the boundary $x=L$, we set $x=L-y$ and obtain

$$\begin{aligned}\frac{f_{L,N}(N-L-1+x;p)}{f_{L,N}(N;p)}&=\left(1-\frac{\gamma_N}{f_{L,N}(N;p)}\sum_{k=0}^{y}\frac{\gamma_{N-k}}{\gamma_N}\right)\\ &=\left(\frac{2\rho}{p}\right)^{y+1}\end{aligned} \tag{4.34}$$

We find that in the low-density phase the density profile decays exponentially with the distance from the blockage (see Fig. 4) on a length scale

$$\xi=\left(\ln\frac{2\rho}{p}\right)^{-1} \tag{4.35}$$

Up to order $1/L$ the profile is given by

$$n(L-y)=\begin{cases}2\rho\left(1-\frac{2}{L}\frac{1-p}{p-2\rho}\right)\left|\sin\left(\frac{\pi}{2}y\right)\right|, & N\leqslant y\leqslant L-1\\ 2\rho\left(1-\frac{2}{L}\frac{1-p}{p-2\rho}\right)\left|\sin\left(\frac{\pi}{2}y\right)\right| & \\ \quad+(1-p)\left(\frac{2\rho}{p}\right)^{y+1}, & 0\leqslant y\leqslant N-1\end{cases} \tag{4.36}$$

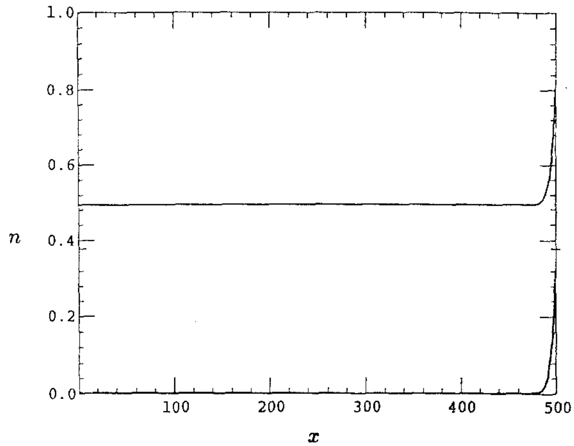

Fig. 4. Density profile in the low-density phase with blockage strength $p=0.6$, $\rho=0.25$, in a chain of 500 sites computed from (4.15). The lower curve is the profile on the even sublattice, the upper curve is the profile on the odd sublattice.

The average density on the even sublattice n^{even} is of order $1/L$:

$$\rho^{\text{even}}=\frac{2}{L}\sum_{y=0}^{L/2-1} n(L-2y)=\frac{2}{L}\frac{2\rho(1-p)}{p-2\rho} \tag{4.37}$$

4.3.2. Phase Transition Line $p=2\rho$. As p approaches 2ρ the inverse decay length $\xi^{-1}=\ln(2\rho/p)$ vanishes. In order to analyze the density profile on the phase transition line, we have to study the behavior of the incomplete β-function (4.9) for L, N large. Define the functions z_r and a_r with $r<\rho$ by

$$z_r^2=L\left[(1-2\rho)\ln\frac{1-2\rho}{(1-p)(1-2r)}+(2\rho-2r)\ln\frac{2\rho-2r}{p(1-2r)}\right]$$
$$-2\ln\frac{(1-2\rho)(2\rho-2r)}{(1-p)(1-2r)^2} \tag{4.38}$$

and

$$a_r=\frac{2}{3}\left(\frac{2}{L}\right)^{1/2}\frac{4\rho-1-r}{[(1-2\rho)(2\rho-2r)(1-2r)]^{1/2}} \tag{4.39}$$

together with the convention that z_r is the positive root of the r.h.s. of (4.38) if $p<(2\rho-2r)/(1-2r)$ and the negative root otherwise. For large L and if $|z_r/a_r|\ll 1$ (if z_r is negative) or if $z_r>0$, the incomplete β-function

$I_{1-p}(L/2-N, N-rL)$ [see (4.9)] is given up to order $L^{1/2}$ by the probability integral

$$P(z_r) = \frac{1}{(2\pi)^{1/2}} \int_{-\infty}^{z_r} e^{-t^2/2}\, dt \tag{4.40}$$

In particular, for $p = 2\rho$ one obtains

$$z_r^2 = L\left[(1-2r) \ln \frac{1}{1-2r} + (2\rho - 2r) \ln \frac{\rho - r}{\rho} \right] - 2 \ln \frac{\rho - r}{\rho(1-2r)^2} \tag{4.41}$$

and z_r negative for $r > 0$. Furthermore, for $r = y/L$, z_r reduces to quantities of order y^2/L, i.e., $z_r = 0$ for finite y in the limit $L \to \infty$:

$$z_{y/L}^2 = \frac{1-2\rho}{\rho} \frac{y^2}{L} + \frac{1-4\rho}{\rho} \frac{2y}{L} \to 0 \tag{4.42}$$

From these considerations we obtain the critical current

$$j_c = p \frac{P(z_0)}{P(z_{-1/L})} = p + O(L^{-1/2}) \tag{4.43}$$

since $P(z_{-1/L}) \approx P(z_0) = P(0) = 1/2$.

Approaching the critical line from the low-density phase and keeping the ratio of the decay length ξ of (4.35) to the size L of the system finite, one obtains in the limit $L \to \infty$

$$z_{y/L}^2 \propto f_{y/L}(\xi/L)\, \xi^{-1} \tag{4.44}$$

Thus the current approaches its critical value as a power law

$$j_c - j \approx p \frac{(z_{-1/L} - z_0) \exp(-z_0^2/2)}{P(z_{-1/L})} \propto \xi^{-1/2} \tag{4.45}$$

Setting $x = L - y$, the density profile is flat for finite y, up to corrections of order $L^{-1/2}$. For large distances, $y = uL^{1/2}$, the profile $n(u)$ is given by

$$\begin{aligned} n(u) &= p \left| \sin\left(\frac{\pi}{2} y\right) \right| + (1-p) \frac{P(z_{y/L})}{P(z_{-1/L})} \\ &= p \left| \sin\left(\frac{\pi}{2} y\right) \right| + (1-p) \left(\frac{2}{\pi}\right)^{1/2} \int_{-\infty}^{-(1-2\rho)u/\rho} e^{-t^2/2}\, dt + O(L^{-1/2}) \end{aligned} \tag{4.46}$$

4.3.3. Coexistence Phase $p < 2\rho$. When $p < 2\rho$ the quantity z_r diverges in the large-L limit to $+\infty$. Therefore one has for some finite (noninfinitesimal) value $r_0 - \Delta$

$$\begin{aligned} P(z_r) &= P(z_{-1/L}) = 1 \qquad (0 < r < r_0 - \Delta) \\ P(z_r) &= 0 \qquad (r_0 + \Delta < r < \rho) \end{aligned} \tag{4.47}$$

with corrections exponentially small in L. For the current we find

$$j = p\,\frac{P(z_{-1/L})}{P(z_0)} = p \tag{4.48}$$

As a result of Eqs. (4.47) there is a low-density region with a flat profile given by

$$n(x) = p\left|\sin\left(\frac{\pi}{2}x\right)\right| \qquad (x < x_0 - \Delta) \tag{4.49}$$

coexisting with a high-density region with flat profile

$$n(x) = p\left|\sin\left(\frac{\pi}{2}x\right)\right| + 1 - p \qquad (x > x_0 + \Delta) \tag{4.50}$$

The interface of width 2Δ between the low- and high-density regions is centered at the distance $L - x_0 = y_0 = Lr_0 = L\rho(1 - s_0)$ from the boundary as determined in the previous subsection. One has $z_{r_0} = 0$; therefore the density profile near y_0 is constant in a finite area around y_0 (up to order $L^{-1/2}$). Choosing $\tilde{x} = y_0 - x = \tilde{u}L^{1/2}$, we obtain the shape of the interface from (4.46) with u replaced by $\tilde{u}$ (see Fig. 5).

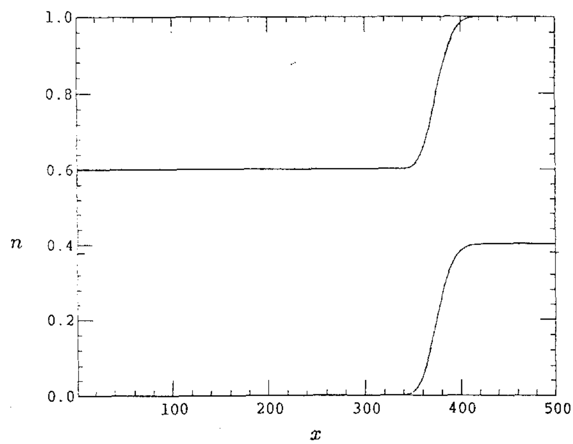

Fig. 5. Density profile in the coexistence phase with blockage strength $p = 0.6$, $\rho = 0.4$, in a chain of 500 sites computed from (4.15). The lower curve is the profile on the even sublattice, the upper curve is the profile on the odd sublattice.

For the width Δ, (4.46) gives

$$\Delta \propto L^{1/2} \qquad (\rho \neq 1/2,\ p \neq 0) \tag{4.51}$$

If $\rho = 1/2$, the approximation (4.40) is not valid. In this case, however, we already know from the density profile (4.19) (for $\rho = 1/2$) obtained in the previous subsection that $\Delta = 0$. The density profile (4.18) in the case $p = 0$ (full blockage) also gives $\Delta = 0$.

4.4. Steady-State Correlation Functions

The rules for the construction of the eigenvectors of the transfer matrix **3A–3D** and Eq. (3.13) contain far-reaching implications also for the (unnormalized) steady-state density correlation functions

$$\mathcal{G}_{L,N}(x_1,..., x_n; p) = \langle 1 |\, \tau_{x_1} \cdots \tau_{x_n} \,| 1 \rangle \tag{4.52}$$

Rule **3A** [see also (A.2) in the Appendix] states that if there is a particle at site $2x$ in a state contributing to the steady state, then *all* odd sites $2x < 2y+1 < 2L$ must also be occupied. This implies for correlation functions of at least one even argument

$$\mathcal{G}_{L,N}(x_1,..., x_n; p) = \mathcal{G}_{L,N}(2y_1 - 1,..., 2y_k - 1, 2y_l,..., 2y_m; p) \tag{4.53}$$

In this expression the set of even sites $\{2y_l,..., 2y_m\}$ denotes all even sites in the set $\{x_1,..., x_n\}$ and $2y_l$ is the lowest one. The set $\{2y_1 - 1,..., 2y_k - 1\}$ are all odd x_i, $x_i \in \{x_1,..., x_n\}$, which are smaller than $2y_l$.

Equation (3.13) relating wave functions with some even arguments to wave functions with only odd arguments and rules **3B–3D** imply more relations on the n-point correlators. Here we focus on the two-point function.

For the two-point function (4.53) reads

$$\mathcal{G}_{L,N}(2x, 2y+1; p) = \mathcal{G}_{L,N}(2x; p) \quad (2 \leqslant 2x < 2y+1 < L) \tag{4.54}$$

Using rules **3B** and **3C** [see also (A.7) and (A.8) in the Appendix] one gets

$$\mathcal{G}_{L,N}(2x-1, 2y; p) = \begin{cases} p\mathcal{G}_{L,N}(2y; p) & (L - N \leqslant 2y \leqslant L - 2x \\ & \qquad \leqslant L-1) \\ 0 & (2y = L - 2x + 2) \end{cases} \tag{4.55}$$

Current conservation finally yields

$$\mathcal{G}_{L,N}(2x-1, 2x; p) = \mathcal{G}_{L,N}(2x-1; p) - j \qquad (1 \leqslant 2x-1 \leqslant L-1) \tag{4.56}$$

The remaining correlator between sites on the even and odd sublattices $\mathscr{G}_{L,N}(2x-1, 2y; p)$ in the range defined by $L-N<2y\leqslant L$ and $L-2y+3 \leqslant 2x-1\leqslant 2y-3$ can be computed like the one-point function from the contribution from the various pairs defined above. The result is

$$\mathscr{G}_{L,N}(2x-1, 2y; p) = (1-p)[pf_{L,N}(N-L+2y-2; p)+f_{L,N}(N-L+2x-2; p)] \tag{4.57}$$

Defining the normalized correlation function by

$$\langle\tau_x\tau_y\rangle = \mathscr{G}_{L,N}(x, y; p)/\mathscr{F}_{L,N}(p) \tag{4.58}$$

we can express all the density correlators (4.54)–(4.57) in terms of the one-point function $\langle\tau_x\rangle = n(x)$ [see (4.14)] in the following way:

$$\langle\tau_{2x-1}\tau_{2y}\rangle = \begin{cases} p\langle\tau_{2y}\rangle & (1\leqslant 2x-1\leqslant L-2y-1) \\ 0 & (2x-1=L-2y+1) \\ \langle\tau_{2y-1}\rangle - j + (1-p) \\ \qquad\times(\langle\tau_{2x-1}\rangle - j) & (L-2y+3\leqslant 2x-1\leqslant 2y-3) \\ \langle\tau_{2y-1}\rangle - j & (2x-1=2y-1) \\ \langle\tau_{2y}\rangle & (2y+1\leqslant 2x-1\leqslant L-1) \end{cases} \tag{4.59}$$

From (3.13) and rule **3D** one obtains for the correlation function on the even sublattice

$$\mathscr{G}_{L,N}(2x, 2y; p) = \begin{cases} (1-p)\,\mathscr{G}_{L,N}(2x; p) & (L-N\leqslant 2x\leqslant L) \\ 0 & (2\leqslant 2x\leqslant L-N-1) \end{cases} \tag{4.60}$$

which implies

$$\langle\tau_{2x}\tau_{2y}\rangle = (1-p)\langle\tau_{2x}\rangle \qquad (2\leqslant 2x\leqslant 2y\leqslant L) \tag{4.61}$$

The remaining correlators are $\mathscr{G}_{L,N}(2x-1, 2y-1; p)$ on the odd sublattice, which can be obtained by counting the contributions from each pair. In range I defined by $1\leqslant 2x-1\leqslant L-2y+1$ the result is

$$\mathscr{G}_{L,N}(2x-1, 2y-1; p) = p^2 f_{L,N}(N-2; p) + p(1-p)f_{L,N}(N-L+2y-2; p) \quad \text{(I)} \tag{4.62}$$

and in range II defined by $L-2y+1<2x-1<2y-1$ one obtains

$$\begin{aligned}\mathscr{G}_{L,N}(2x-1, 2y-1; p) &= p^2 f_{L,N}(N-2; p) + p(1-p)f_{L,N}(N-L+2y-3; p) \\ &\quad + (1-p)f_{L,N}(N-L+2x-2; p) \qquad \text{(II)}\end{aligned} \tag{4.63}$$

Thus also the density correlation function involving two odd lattice sites can be expressed in terms of the one-point function and another constant

$$\alpha^2 = f_{L,N}(N-2; p)/\mathscr{F}_{L,N}(p) \tag{4.64}$$

We obtain

$$\langle \tau_{2x-1}\tau_{2y-1}\rangle = \begin{cases} p^2\alpha^2 + p(\langle \tau_{2y-1}\rangle - j) & (1 \leqslant 2x-1 \leqslant L-2y+1) \\ p^2\alpha^2 + p\langle \tau_{2y-2}\rangle & \\ \quad + \langle \tau_{2x-1}\rangle - j & (L-2y+1 < 2x-1 < 2y-1) \end{cases} \tag{4.65}$$

These relations allow us to obtain simple exact expressions for the connected two-point function

$$n(x_1, x_2) = \langle \tau_{x_1}\tau_{x_2}\rangle - \langle \tau_{x_1}\rangle\langle \tau_{x_2}\rangle \tag{4.66}$$

and their large-L behavior. On the even sublattice (4.61) gives

$$n(2x_1, 2x_2) = n(2x_1)[1 - p - n(2x_2)] \qquad (2x_2 > 2x_1) \tag{4.67}$$

If the system is in the low-density phase, the density $n(L-2y)$ decays exponentially with increasing distance $2y$ from the boundary [cf. (4.34)]. Defining the relative distance r by $r = 2x_2 - 2x_1 > 0$, we obtain for L large

$$\begin{aligned} n(L-2y_1, L-2y_2) &= (1-p)^2 \left(\frac{2\rho}{p}\right)^{2y_1+1} \left[1 - \left(\frac{2\rho}{p}\right)^{2y_2+1}\right] \\ &= A(y_2)\, e^{-r/\xi} \end{aligned} \tag{4.68}$$

with the decay length ξ of (4.35) as correlation length and a space-dependent amplitude

$$A(y_2) = (1-p)^2\, e^{-(2y_2+1)/\xi}(1 - e^{-(2y_2+1)/\xi}) \tag{4.69}$$

On the phase transition line and in the coexistence phase one has in the large-L limit $n(L-2y_1) = n(L-2y_2)$ for finite distance r. Here the connected two-point correlation function does not depend on r:

$$n(L-2y_1, L-2y_2) = \tilde{A}(y_2) \tag{4.70}$$

with

$$\tilde{A}(y_2) = n(L-2y_2)[1 - p - n(L-2y_2)] \tag{4.71}$$

(The finite-size corrections are of order $L^{-1/2}$.) We conclude that in the thermodynamic limit the connected density–density correlation function on the even sublattice is of a generalized scaling form

$$n(x_1, x_2) = A(x_2)\, r^{\kappa} e^{-r/\xi} \tag{4.72}$$

with a critical exponent $\kappa = 0$ and a space-dependent amplitude A. In the low-density phase A is nonvanishing only close to the boundary. On the phase transition line and in the coexistence phase one has $\xi = \infty$ and the amplitude is nonzero in a boundary region of width of order $L^{1/2}$ or in the interface, respectively. In this sense the boundary region (or the interface, respectively) is a critical region in the system. The correlation function vanishes if either of the two points is well inside the low- or high-density regions, independent of the phase.

Since the model is defined on a ring, one may ask whether there are correlations between points close to the right and close to the left of the boundary. For the even sublattice the answer is easy to find from the exact expression (4.67), which shows that the connected correlation function is 0 for $2 \leqslant 2x_1 \leqslant L - N$ and $2x_2 > 2x_1$.

For the other connected correlation functions (involving even and odd or only odd sites) one obtains similar results. There is one difference, however: the density on the odd sublattice close to the right of the boundary (small $2x - 1$) is correlated with the density on the even and odd sublattices close to the left (high $2y$ or $2y - 1$, respectively) if the system is in the low-density phase. Setting $x_1 = 2x - 1$, $x_2 = L - 2y$, or $x_2 = L - 2y + 1$, one obtains in the region defined by $L - N < x_2 \leqslant L$ and $1 \leqslant x_1 < L - x_2$

$$n(x_1, x_2) = (p^2\alpha^2 - pj) \left| \sin\left(\frac{\pi}{2} x_2\right) \right| + n(x_2)[p - n(x_1)] \tag{4.73}$$

On the phase transition line and in the coexistence region one has in the thermodynamic limit $\alpha = 1$ and $n(x_1) = p$ and therefore $n(x_1, x_2) = 0$. In the low-density region one finds $\alpha = 2\rho/p$ and $n(x_1) = 2\rho$. This yields

$$n(x_1, x_2) = 2\rho(1 - p)\left(1 - \frac{2\rho}{p}\right) e^{-(L - x_2)/\xi} \tag{4.74}$$

This correlation function seems to be independent of x_1, but note that this expression is valid only in the range $1 \leqslant x_1 < L - x_2$. There is a discontinuity at $x_1 = L + 1 - x_2$ [see the exact expressions (4.59) and (4.65)] beyond which this correlation function vanishes even in the low-density phase.

5. COMPARISON WITH OTHER MODELS AND CONCLUSIONS

We have solved and studied a one-dimensional asymmetric exclusion process with a blockage equivalent to a two-dimensional vertex model with a defect line. The symmetries of the system are such that the subspace of states with nonzero eigenvalue of the transfer matrix is much smaller than its dimension. This enabled us to generalize the Bethe ansatz (3.3) by restricting it to this subspace in a suitably chosen basis defined by (3.13) and rules **3A–3D** and by choosing boundary conditions on the wave function appropriately [see (3.17)]. This is the first main result of this paper. The fact that the model can be solved by Bethe ansatz methods is somewhat surprising because the defect-type boundary conditions considered here do not belong to the known classes of integrable boundary conditions. So one can ask whether also certain higher vertex models corresponding to multiparticle systems[2,9,14] with a defect line might be soluble by similar generalizations of the Bethe ansatz. It would be particularly interesting to know if the asymmetric exclusion process solved by Gwa and Spohn[12] with the Bethe ansatz for periodic boundary conditions remains integrable if a blockage-type defect is introduced. This would correspond to the model studied numerically by Janowsky and Leibowitz.[8]

Given the Bethe solution, we presented a detailed study of the steady state of the model considered as a one-dimensional chain of particles moving around the ring with a blockage of strength p at the boundary connecting sites L and 1. We computed exact expressions for the current j, the average occupation number $n(x)$, and the two-point correlation functions $n(x, y)$ as functions of x, y, and p for any number of particles N and any length L of the chain. This is the second main result, [see Eqs. (4.14), (4.15), (4.61), (4.59), and (4.65)]. The average occupation numbers $n(x)$ on the even and the odd sublattices differ by a constant which is the current j flowing in the system. We established the presence of phase transitions from a low-density phase to a coexistence phase at the critical density $\rho_{\text{crit}} = p/2$ and by the particle–hole symmetry (2.9) from the coexistence phase to a high-density phase at density $\tilde{\rho}_{\text{crit}} = 1 - p/2$. The phase diagram is given in Fig. 2 in the density–blockage plane and in Fig. 3 in the current–blockage plane.

In the continuum limit $L \to \infty$, $\rho = N/L$ fixed, the rescaled density profile is asymptotically constant in the low-density phase (I) $\rho < \rho_{\text{crit}}$. On the odd sublattice one has $n(2x-1) = \rho^{\text{odd}} = 2\rho$, while on the even sublattice $\rho^{\text{even}} = 0$. The current j increases with ρ as $j = 2\rho$. In the coexistence phase there are two regions of different constant density. Taking the average densities of the even and odd sublattices, one finds $\tilde{\rho}_{\text{crit}} =$

$\rho_{\text{left}} = 1 - \rho_{\text{right}} = 1 - \rho_{\text{crit}}$ and $j = p$. In the (asymptotically) uniform high-density phase $\rho > \tilde{\rho}_{\text{crit}}$ the densities are given by $\rho^{\text{odd}} = 1$ and $\rho^{\text{even}} = 2\rho - 1$ and $j = 2(1 - \rho)$.

This phase diagram is qualitatively similar to one found numerically by Janowsky and Lebowitz[8] in a different model. They considered a fully asymmetric exclusion process with blockage and, as opposed to the case considered here, probabilistic movement of particles also in the bulk. In this case the dependence $j(\rho)$ is different and one cannot expect ρ_{crit} as a function of the blockage strength to be the same. Relations (4.30) determining the average density profile in the continuum limit, however, do coincide. Whether the motion of particles in the bulk is deterministic or not does not seem to have much influence on the phase diagram.

Studying large but finite systems, we observed in the low-density phase an exponential decay of the density profile near the blockage on a length scale ξ [see Eq. (4.35)]. The connected two-point correlation function is of a generalized scaling form $n(x, y) = A(y)\, r^{\kappa} e^{-r/\xi}$ [Eq. (4.72)] with a space-dependent amplitude A and $\kappa = 0$. On approaching the phase transition line, ξ diverges (in the thermodynamic limit) and the current reaches its critical value p as a power law, (4.45).. In phase II the profile near the blockage is flat. The amplitude of the correlation function is nonvanishing only in the interface between the low-density region and the high-density region. In this area the correlation function is constant for finite distances r, but the amplitude is space dependent. The width of the interface grows as $L^{1/2}$ with the size L of the system if $\rho \neq 1/2$ and is 0 if $\rho = 1/2$. In the dynamical picture of the model the blockage causes particles to pile up and to introduce a shock into the stationary state. Our analysis shows that the fluctuations in the position of the shock (which corresponds to the width of the interface) scale as $L^{1/2}$ if ρ is not infinitesimally close to 0 or 1/2. If $\rho = 1/2$, however, the dimension of the subspace spanned by eigenvectors with nonzero eigenvalues of the transfer matrix is only one-dimensional; the steady state is the only relevant state. So there are no relevant fluctuations and correspondingly no fluctuations in the shock position. These two kinds of scaling behavior support the hypothesis of Janowsky and Lebowitz[8] separating the fluctuations into a part originating in the "blockage randomness" (causing the $L^{1/2}$ law) and into a part originating in the "dynamical randomness" caused by the random movement of the particles in the bulk, which is absent in our model and therefore does *not* generate a $L^{1/3}$ behavior if $\rho = 1/2$ as in ref. 8. The flatness of the density profile near the blockage found in our model is not observed in ref. 8, where numerical analysis suggests that the profile decays as $1/(y - c)$ to the value ρ_{left} with distance y from the blockage. We suggest that there are nonvanishing density correlations close to the boundary even in the coexistence phase which produce this effect. They are absent in our model, where the motion of particles is deterministic.

In order to get some insight in the influence of the boundary conditions on the phase diagram, we would like to compare the model discussed here with similar models but other boundary conditions. Recently Derrida *et al.*[15] solved a fully probabilistic asymmetric exclusion process with open boundary conditions and injection of particles with rate α at one end of the chain and annihilation with rate β at the other end. Here the phase diagram has a richer structure. In addition to the low- and high-density phases and the coexistence phase there is a maximal current phase where the current takes its maximal value independent of α and β. In this phase the density profile near the origin (where particles are injected) decays as $x^{-1/2}$ with distance x to its bulk value 1/2. It would be very interesting to study the deterministic model presented in this paper with this kind of boundary condition.

Appendix. THE INVARIANT SUBSPACE OF $T(p)$

Here we prove rules **3A–3D** and Eq. (3.13) defining an invariant right subspace of $T(p)$ of dimension

$$d_N(L) = \binom{L/2}{N} \qquad (0 \leqslant N \leqslant L/2) \tag{A.1}$$

Rule **3A** can be written as

$$\tau_{2x}\sigma_{2y+1}\,|\Lambda\rangle = 0 \qquad (\Lambda \neq 0) \tag{A.2}$$

with the restriction $2 \leqslant 2x < 2y+1 \leqslant L-1$. First note that from the commutation relations (2.12) we immediately obtain

$$(\tau_{2x} - \tau_{2x}\tau_{2x+1})\,T(p) = \tau_{2x}\sigma_{2x+1}T(p) = 0 \qquad (x \neq L/2) \tag{A.3}$$

and

$$\begin{aligned} \tau_{2x}\sigma_{2x+3}T(p) &= T(p)(1-\sigma_{2x-1}\sigma_{2x})\,\tau_{2x+1}\tau_{2x+2}\sigma_{2x+1}\sigma_{2x+2}(1-\tau_{2x+3}\tau_{2x+4}) \\ &= 0 \qquad (x \neq L/2-1,\, L/2) \end{aligned} \tag{A.4}$$

Acting with $\tau_{2x}\sigma_{2x+1}T(p)$ or $\tau_{2x}\sigma_{2x+3}T(p)$ on an eigenstate of $T(p)$ therefore gives 0, implying that in eigenstates with nonzero eigenvalue the amplitude of a configuration with a particle on site $2x$ and a hole on site $2x+1$ or site $2x+3$ must be zero. Furthermore, one obtains $(2 \leqslant 2x < 2y+1 \leqslant L-1)$

$$\tau_{2x}\sigma_{2y+1}T(p) = T(p)(1-\sigma_{2x-1}\sigma_{2x})\,\tau_{2x+1}\tau_{2x+2}\sigma_{2y-1}\sigma_{2y}(1-\tau_{2y+1}\tau_{2y+2}) \tag{A.5}$$

Acting with $\tau_{2x}\sigma_{2y+1}T(p)$ on an eigenstate with nonzero eigenvalue proves **3A** by induction.

The restriction $2y+1 \leqslant L-1$ arises from the defect at the boundary, where the analogue to (A.3) reads

$$\tau_L\sigma_1 T(p) = (1-p)\,T^F(1-\sigma_{L-1}\sigma_L)(1-\tau_1\tau_2) \tag{A.6}$$

If $p=1$ (no blockage), the r.h.s. of this equation is zero and consequently there is no restriction on $2x$ and $2y+1$ in **3A**. If $N \leqslant L/2$, this implies $\tau_{2x}\,|\Lambda\rangle = 0$.

Rule **3B** reads

$$\tau_{2x}\tau_{L+1-2x}\,|\Lambda\rangle = 0 \qquad (\Lambda \neq 0) \tag{A.7}$$

with $1 \leqslant x \leqslant L/2$ and rule **3C** states

$$\tau_{2x}\sigma_{2y+1}\sigma_{L-2y}\,|\Lambda\rangle = 0 \qquad (\Lambda \neq 0) \tag{A.8}$$

We start by proving rule **3B** with $2x=L$ and $2x=L-2$. From the boundary commutators (2.13) we obtain

$$\tau_L\tau_1 T(p) = T(p)(1-\sigma_{L-1}\sigma_L)\,\tau_1\tau_2 \tag{A.9}$$

Suppose $N \leqslant L/2$ and $|\Lambda\rangle$ contains a state with particles on sites 1 and 2 (so that $\tau_1\tau_2\,|\Lambda\rangle \neq 0$). Then according to **3A** this state cannot have a hole on any odd site $3 \leqslant 2y+1 \leqslant L-1$, i.e., it must have at least $L/2+1$ particles, in contradiction to the assumption $N \leqslant L/2$. Therefore $\tau_1\tau_2\,|\Lambda\rangle = 0$ and consequently according to (A.9) $\tau_L\tau_1\,|\Lambda\rangle = 0$ if $\Lambda \neq 0$. Using this result, one proves in a similar manner $\tau_{L-2}\tau_3\,|\Lambda\rangle = 0$ if $\Lambda \neq 0$.

Having established the validity of **3B** in this special case, we can prove rule **3C** with $2y+1=1$ and $2y+1=3$, $2 \leqslant 2x < L-2y$ arbitrary. First note that

$$\tau_{2x}\sigma_1\sigma_L\,|\Lambda\rangle = \tau_{2x}(1-\tau_L-\tau_1-\tau_L\tau_1)\,|\Lambda\rangle = \tau_{2x}(1-\tau_L-\tau_1)\,|\Lambda\rangle$$

Then the commutators (2.12) and (2.13) give

$$\tau_{2x}(1-\tau_L-\tau_1)\,T(p) = T(p)(1-\sigma_{2x-1}\sigma_{2x})\,\tau_{2x+1}\tau_{2x+2}(\sigma_{L-1}\sigma_L-\tau_1\tau_2) \tag{A.10}$$

Acting with the r.h.s. of this equation on an eigenstate with $\Lambda \neq 0$ gives zero according to what has been proven so far; therefore $\tau_{2x}\sigma_1\sigma_L |\Lambda\rangle = 0$. Again similar arguments lead to $\tau_{2x}\sigma_3\sigma_{L-2} |\Lambda\rangle = 0$ and from these results rules **3B** and **3C** follow by induction.

Rule **3D** is a simple consequence of **3A**–**3C**: Suppose a state with a particle on site $2x$ has a nonzero amplitude in an eigenstate of $T(p)$. Then according to rule **3A** all odd sites larger than $2x$ up to site $L-1$ must be occupied, too, and in addition to that each *even* site $2y$, $L \geqslant 2y > 2x$, or its reflected *odd* counterpart $L+1-2y$ must contain a particle (see **3B** and **3C**). Since $N \leqslant L/2$, rule **3D** follows.

Now we are in a position to prove (3.13) relating wave functions with some even arguments to wave functions with odd arguments only. Define the operator $\tau(x_1,..., x_m)$ by

$$\tau(x_1,..., x_m) = \prod_{i=1}^{m} \tau_{x_i} \tag{A.11}$$

Since the left eigenvector to eigenvalue 1 is the sum of all N-particle states with equal weight $\Phi = 1$ (independent of p), one finds for the (unnormalized) right wave function

$$\Psi_\Lambda(x_1,..., x_N) = \langle 1| \tau(x_1,..., x_N) |\Lambda\rangle \tag{A.12}$$

In particular, using rules **3A**–**3D** and the boundary commutators (2.13), one obtains for $2 \leqslant x_i \leqslant L-1$

$$\begin{aligned}\Lambda\Psi_\Lambda(1, x_1,..., x_{N-1}) &= \langle 1| \tau_1\tau(x_1,..., x_{N-1})\, T(p) |\Lambda\rangle \\ &= p\langle 1| \tau(x_1,..., x_{N-1})\, T^P(1-\sigma_{L-1}\sigma_L) |\Lambda\rangle \\ &= p\langle 1| \tau(x_1,..., x_{N-1})\, T(p)(1-\sigma_{L-1}\sigma_L) |\Lambda\rangle\end{aligned} \tag{A.13}$$

The last equation is due to the fact that acting first with τ to the *left* projects out all states with particles on sites L and 1. Acting then with T to the left again does not depend on p and we can substitute T^P by $T(p)$. On the other hand, one gets

$$\begin{aligned}&\Lambda\Psi_\Lambda(x_1,..., x_{N-1}, L) \\ &\quad = \langle 1| \tau_L\tau(x_1,..., x_{N-1})\, T(p) |\Lambda\rangle \\ &\quad = (1-p)\langle 1| \tau(x_1,..., x_{N-1})\, T^F(1-\sigma_{L-1}\sigma_L) |\Lambda\rangle \\ &\quad = (1-p)\langle 1| \tau(x_1,..., x_{N-1})\, T(p)(1-\sigma_{L-1}\sigma_L) |\Lambda\rangle\end{aligned} \tag{A.14}$$

As a result, if $\Lambda \neq 0$, we conclude

$$\Psi_\Lambda(x_1,..., x_{N-1}, L) = \frac{1-p}{p}\, \Psi_\Lambda(1, x_1,..., x_{N-1}) \tag{A.15}$$

and (3.13) follows by induction. Rules **3A–3D** select a set of configurations that contribute to the relevant eigenvectors of $T(p)$. The number of these configurations is clearly larger than $d_N(L)$ [see (A.1)] if $p \neq 0, 1$, but (3.13) states that the amplitudes of configurations with particles on even sites are in a fixed relationship (i.e., independent of the particular eigenvector) with the amplitudes of exclusively odd configurations. This reduces the number of linear independent configurations in this subspace to $d_N(L)$, as stated above.

ACKNOWLEDGMENTS

It is a pleasure to thank E. Domany for bringing to my attention refs. 3, 8, and 15, which triggered this work. I also thank him and D. Mukamel for stimulating discussions. Financial support by the Minerva Foundation is gratefully acknowledged.

REFERENCES

1. R. J. Baxter, *Exactly Solved Models in Statistical Mechanics* (Academic Press, New York, 1982).
2. H. J. de Vega, *Int. J. Mod. Phys.* **4**:2371 (1989); H. J. de Vega, *Nucl. Phys. B (Proc. Suppl.)* **18A**:229 (1990).
3. D. Kandel, E. Domany, and B. Nienhuis, *J. Phys. A* **23**:L755 (1990).
4. T. M. Ligget, *Interacting Particle Systems* (Springer-Verlag, New York, 1985).
5. R. Kutner, *Phys. Lett. A* **81**:239 (1981); H. van Beijeren, K. W. Kehr, and R. Kutner, *Phys. Rev. B* **28**:5711 (1983); P. A. Ferrari, *Ann. Prob.* **14**:1277 (1986); A. De Masi and P. Ferrari, *J. Stat. Phys.* **36**:81 (1984); J. P. Marchand and P. A. Martin, *J. Stat. Phys.* **44**:491 (1986); D. Kandel and E. Domany, *J. Stat. Phys.* **58**:685 (1990).
6. J. Krug and H. Spohn, in *Solids far from Equilibrium: Growth, Morphology and Defects*, C. Godreche, ed. (Cambridge University Press, Cambridge, 1991).
7. M. Kardar, G. Parisi, and Y. Zhang, *Phys. Rev. Lett.* **56**:889 (1986).
8. S. A. Janowsky and J. L. Lebowitz, *Phys. Rev. A* **45**:618 (1992).
9. D. Kandel and D. Mukamel, *Phys. Rev. Lett.*, submitted.
10. J. Krug, *Phys. Rev. Lett.* **61**:1882 (1991).
11. E. K. Sklyanin, *J. Phys. A* **21**:2375 (1988).
12. L.-H. Gwa and H. Spohn, *Phys. Rev. Lett.* **68**:725 (1992); *Phys. Rev. A* **46**:844 (1992).
13. C. Destri and H. J. de Vega, *Nucl. Phys. B* **290**:363 (1987).
14. B. Sutherland, *Phys. Rev. B* **12**:3795 (1975).
15. B. Derrida, E. Domany, and D. Mukamel, preprint (1992).